

## Stochastic modeling in lithography: autocorrelation behavior of catalytic reaction–diffusion systems

**Chris A. Mack**  
1605 Watchhill Road  
Austin, Texas, 78703

**Abstract.** Reaction–diffusion chemical systems where the catalyst of the reaction is the only diffusing species are investigated. Here, the correlation length and Hurst roughness exponent are derived in one-, two-, and three-dimensional first-order catalytic reaction–diffusion problems. These results are relevant to many chemical systems, and in particular to chemically amplified photoresists used in semiconductor lithography, where the correlation length and Hurst exponent affect the line-edge roughness of sub-100-nm printed features. © 2009 Society of Photo-Optical Instrumentation Engineers. [DOI: 10.1117/1.3155516]

Subject terms: line-edge roughness; reaction-diffusion; correlation length; roughness exponent; Hurst exponent; autocorrelation; stochastic modeling.

Paper 09027CR received Mar. 2, 2009; revised manuscript received Apr. 21, 2009; accepted for publication Apr. 30, 2009; published online Jun. 18, 2009. This paper is a revision of a paper that appeared at the SPIE Conference on Advances in Resist Materials and Processing Technology XXVI, February 2009, San Jose, California. The paper presented there appears (unrefereed) in SPIE Proceedings Vol. 7273.

The stochastic behavior of reaction–diffusion chemical systems, where chemical species are simultaneously reacting and diffusing, has been extensively studied.<sup>1</sup> Unfortunately, analytic solutions to the stochastic differential equations governing these systems are rarely available, and so numerical simulations are frequently employed.<sup>2</sup> Still, there is a need for simple analytical descriptions of key phenomenon, to provide insight and to validate and guide model development.

An important class of reaction–diffusion problems is that of a diffusing catalyst with all other reactants immobile. As an example, consider chemically amplified photoresists used in semiconductor lithography. Exposure of the polymer-based resist to light causes the generation of acid. A subsequent bake step allows the acid to diffuse and cause chemical reactions at specific sites on the surrounding polymer molecules that change their solubility in developer. Since the acid is not consumed in the reaction, it acts as a catalyst. This acid–polymer reaction is first order in acid concentration ( $H$ ) and first order in concentration of reac-

tive polymer sites ( $M$ ), so that the governing kinetic rate equations are

$$\frac{\partial M}{\partial t} = -kMH, \quad \frac{\partial H}{\partial t} = \nabla(D \nabla H), \quad (1)$$

where  $k$  is the reaction rate constant, and  $D$  is the acid (catalyst) diffusivity. Of course, these reaction–diffusion rate equations apply to many other catalytic systems as well.

Mean-field solutions to the reaction–diffusion system of Eq. (1) are useful in higher-dimensional problems (for example, Euclidian dimension  $d=3$ ), when the size of the domain of interest is large enough to ignore stochastic variations. In sub-100-nm lithography, however, stochastic variations give rise to roughness at the edges of the printed features with RMS edge deviations of several nanometers.<sup>3–6</sup> Further, frequency analysis of this roughness shows correlation lengths that can be tens of nanometers.<sup>4,5</sup> It is the goal of this work to derive the autocorrelation behavior of first-order two-component reaction–diffusion systems where the only diffusing component is a catalyst.

Solving the mean-field reaction kinetic equation gives

$$\frac{\langle M \rangle}{M_0} = \exp(-kt \langle H_{eff} \rangle), \quad (2)$$

where  $M_0$  is the initial concentration of  $M$ , and  $H_{eff}$  is the effective catalyst concentration, the time average of the catalyst concentration experienced by a reaction site. The effective catalyst concentration can be calculated from,<sup>3</sup>

$$H_{eff} = H(t=0) \otimes R_{PSF} \text{ and } \langle H_{eff} \rangle = \langle H(t=0) \rangle \otimes R_{PSF}, \quad (3)$$

where  $\otimes$  denotes convolution, and the reaction–diffusion point spread function ( $R_{PSF}$ ) is the time average of the diffusion point spread function ( $D_{PSF}$ ):

$$R_{PSF} = \frac{1}{t_f} \int_0^{t_f} D_{PSF} dt, \quad (4)$$

where  $t_f$  is the total reaction–diffusion time. For the case of constant diffusivity of the catalyst, the  $D_{PSF}$  is the standard Gaussian diffusion kernel and is affected by time integration through the diffusion length,  $\sigma_D = (2Dt)^{1/2}$ . Thus, using the 1-D case as an example,

$$R_{PSF} = \frac{1}{t_f \sqrt{4\pi D}} \int_0^{t_f} \frac{\exp(-x^2/4Dt)}{\sqrt{t}} dt. \quad (5)$$

Analytic expressions for  $R_{PSF}$  have been previously derived for 1-D, 2-D, and 3-D cases.<sup>3</sup>

$$\begin{aligned}
\text{1-D: } R_{PSF}(x) &= 2 \frac{\exp(-x^2/2\sigma_D^2)}{\sqrt{2\pi}\sigma_D} - \frac{|x|}{\sigma_D^2} \operatorname{erfc}\left(\frac{|x|}{\sqrt{2}\sigma_D}\right), \\
\text{2-D: } R_{PSF}(r) &= -\frac{1}{\pi\sigma_D^2} \operatorname{Ei}\left(-\frac{r^2}{2\sigma_D^2}\right), \quad r = (x^2 + y^2)^{1/2}, \\
\text{3-D: } R_{PSF}(r) &= \frac{1}{2\pi\sigma_D^3} \left[ \frac{\sigma_D}{|r|} \operatorname{erfc}\left(\frac{|r|}{\sqrt{2}\sigma_D}\right) \right], \\
&\quad r = (x^2 + y^2 + z^2)^{1/2}, \tag{6}
\end{aligned}$$

where  $\operatorname{erfc}$  is the complimentary error function and  $\operatorname{Ei}$  is the exponential integral.

Because a single catalyst molecule diffuses and potentially causes many reactions, these reactions will be stochastically correlated. If the diffusion of the catalyst is the only mechanism by which the concentration  $M$  becomes spatially correlated, the autocorrelation of the  $R_{PSF}$  will define this spatial correlation. Consider first the (non-normalized) autocorrelation of the effective catalyst concentration:

$$R_{H_{eff}}(\tau) \equiv \langle [H_{eff}(r) - \langle H_{eff} \rangle][H_{eff}(r + \tau) - \langle H_{eff} \rangle] \rangle. \tag{7}$$

Applying Eq. (3),

$$R_{H_{eff}} = [(H - \langle H \rangle) \otimes (H - \langle H \rangle)] \otimes [R_{PSF} \otimes R_{PSF}]. \tag{8}$$

Assuming that the initial distribution of the catalyst is stochastically uncorrelated,  $(H - \langle H \rangle) \otimes (H - \langle H \rangle)$  will be a delta function at the origin multiplied by the variance of  $H$ . Thus, for this case,

$$R_{H_{eff}} = \sigma_H^2 (R_{PSF} \otimes R_{PSF}). \tag{9}$$

It will be useful to normalize the autocorrelation function to be one at the origin. For the 1-D case,

$$\tilde{R}_{H_{eff}}(\tau) = \frac{\int_{-\infty}^{\infty} R_{PSF}(x) R_{PSF}(x + \tau) dx}{\int_{-\infty}^{\infty} [R_{PSF}(x)]^2 dx}. \tag{10}$$

For the 2-D and 3-D cases, integrations are best done in polar and spherical coordinates, respectively. This allows the double and triple integrals, respectively, to become single integrals over distance  $r$  [of the form of Eq. (10)] by multiplying the 2-D  $R_{PSF}$  by  $\sqrt{|r|}$  and the 3-D  $R_{PSF}$  by  $|r|$ . Analytical evaluation of Eq. (10) for the 1-D, 2-D, and 3-D cases does not seem possible, so numerical integrations were performed. Figure 1 shows the results. Each of these results can be extremely well approximated by a standard exponential correlation function:

$$\tilde{R}_{H_{eff}}(\tau) = \exp[-(|\tau|/\zeta)^{2\alpha}], \tag{11}$$

where  $\zeta$  is the correlation length, and  $\alpha$  is the Hurst (roughness) exponent. Fitting the numerical evaluation of Eq. (10) to the empirical function (11) produces the results shown in Table 1, where both a linear fit to the autocorrelation function and to the logarithm of the autocorrelation function were performed. The resulting fits are extremely good—plotting the linear fits on Fig. 1 would produce lines indis-

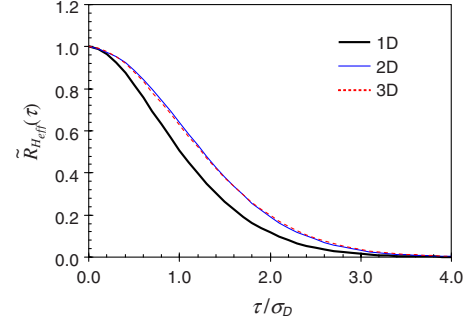


**Fig. 1** Numerical evaluation of the  $R_{PSF}$  autocorrelation for the 1-D (thick solid line), 2-D (thin solid line), and 3-D (dashed line) cases.

tinguishable from the calculated results from Eq. (10). Obviously, the linear fit does a better job of matching the small- $\tau$  behavior, while logarithmic fitting results in better matching to the large- $\tau$  region.

These results show that diffusion of the catalyst in a first-order reaction-diffusion system produces persistent correlation ( $\alpha > 0.5$ ), with a correlation length that is a multiple of the diffusion length (as expected). For the important 3-D case,  $\alpha \approx 0.9$ , and the correlation length is just over 50% greater than the catalyst diffusion length. Note that the correlation length derived here differs significantly from the value of  $\sim \sigma_D/2$  derived by Gallatin.<sup>7</sup>

To find the autocorrelation behavior of the overall reaction, define the relative reaction product concentration as

$$p = 1 - \frac{M}{M_0} = 1 - \exp(-ktH_{eff}). \tag{12}$$

For the chemically amplified resist case,  $p$  represents the relative concentration of deblocked (deprotected) sites. For small amounts of deprotection,

$$p \approx ktH_{eff}, \tag{13}$$

so that the normalized autocorrelation of  $p$  in this regime is

$$\tilde{R}_p(\tau) \approx \tilde{R}_{H_{eff}}(\tau). \tag{14}$$

These results can now be compared to experimental line-edge roughness measurements of printed optical lithography patterns. Measurements of many lithographic patterns for a particular extreme ultraviolet (EUV) lithog-

**Table 1** Results of the best fit of Eq. (11) to the numerically evaluated Eq. (10), using a least-squares fit to  $\tilde{R}_{H_{eff}}$  (linear fit) or to its logarithm (logarithmic fit).

	Linear fit		Logarithmic fit	
	$\zeta/\sigma_D$	$\alpha$	$\zeta/\sigma_D$	$\alpha$
1-D	1.266	0.848	1.252	0.817
2-D	1.532	0.936	1.515	0.901
3-D	1.528	0.900	1.519	0.879

raphy tool showed roughness exponents of about 0.5 to 0.6 and correlation lengths of about 20 nm (Ref. 4), and a 193-nm-wavelength lithography process showed roughness exponents of about 0.4 to 0.6 and correlation lengths of about 20 to 35 nm (Ref. 5). A separate experimental study found a roughness exponent near 0.5 for both electron-beam and 193-nm-wavelength imaging.<sup>6</sup> All of these studies employed chemically amplified resists that follow the basic kinetics described here. The fact that the experimental Hurst exponents are significantly lower than that derived here for the catalytic reaction–diffusion phenomenon suggests that a different correlation mechanism may also be at work. In particular, loss of the acid catalyst through quenching by a diffusing base (an  $A+B\rightarrow 0$  annihilation reaction) is likely to be a significant factor in these resists. Also, dissolution of the polymeric resist is likely to lead to self-affine surfaces with a correlation length dependent on the development time and a roughness exponent closer to the experimentally determined values.<sup>8</sup> Both of these effects need further investigation. It is entirely possible, however, that measurement of the roughness coefficient as previously reported is inaccurate due to the resolution/noise limits of the LER measurements themselves.

In conclusion, numerical evaluation of the analytic reaction–diffusion mechanism for the case of a diffusing

catalyst (in the absence of base quencher) has produced a predicted roughness coefficient intrinsic to this system and a correlation length that is a simple multiple of the diffusion length of the catalyst (in 3-D,  $\alpha \approx 0.9$  and  $\zeta \approx 1.52\sigma_D$ ). These results will be useful in the development of a full stochastic model of LER formation in semiconductor lithography.

## References

1. D. ben-Avraham and S. Havlin, *Diffusion and Reactions in Fractals and Disordered Systems*, Cambridge University Press, Cambridge, UK (2000).
2. T. Mulders, W. Henke, K. Elian, C. Nolscher, and M. Sebal, “New stochastic post-exposure bake simulation method,” *J. Microlithogr., Microsyst.* **4**(4), 043010 (2005).
3. C. A. Mack, *Fundamental Principles of Optical Lithography: The Science of Microfabrication*, John Wiley & Sons, London (2007).
4. P. P. Naulleau and J. P. Cain, “Experimental and model-based study of the robustness of line-edge roughness metric extraction in the presence of noise,” *J. Vac. Sci. Technol. B* **25**, 1647–1657 (2007).
5. L. H. A. Leunissen, W. G. Lawrence, and M. Ercken, “Line edge roughness: experimental results related to a two-parameter model,” *Microelectron. Eng.* **73–74**, 265–270 (2004).
6. A. Yamaguchi and O. Komuro, “Characterization of line edge roughness in resist patterns by using fourier and auto-correlation function,” *Jpn. J. Appl. Phys., Part 1* **42**, 3763–3770 (2003).
7. G. Gallatin, “Resist blur and line edge roughness,” *Proc. SPIE* **5754**, 38–52 (2005).
8. C. A. Mack, “Stochastic modeling in lithography: the use of dynamical scaling in photoresist development,” *J. Micro/Nanolith. MEMS MOEMS* **8** (2009) (accepted).